

Exchanges of Atmospheric CO₂ and ¹³C/12C with the Terrestrial Biosphere and Oceans from 1978 to 2000.

IV. Critical Overview

Charles D. Keeling¹ and Stephen C. Piper¹

Abstract—Interannual variations from 1981 through 1999 in the sources and sinks of atmospheric CO₂ are inferred by a three-dimensional tracer inversion model from simultaneous measurements of the concentration and ¹³C/¹²C isotopic ratio of atmospheric CO₂. Terrestrial exchange of CO₂ with the atmosphere range from -0.9 to +1.6 PgC yr⁻¹ in the northern polar zone, -3.1 to +0.2 PgC yr⁻¹ in the north temperate zone, -2.3 to +6.7 PgC yr⁻¹ in the tropics, and -2.1 to +0.8 PgC yr⁻¹ in the southern temperate zone. Oceanic exchange shows relatively little interannual variability, except in the tropics where a weak sink, up to -0.6 PgC yr⁻¹ during El Niño events in 1983, 1987, and 1998, alternated with a source, as great as 1.7 PgC yr⁻¹. If isotopic data are disregarded as an indicator of interannual variability, inferred fluxes are altered only slightly in the polar and temperate zones, but substantially reduced in the tropical zone to a minimum sink of -0.2 PgC yr⁻¹ and a maximum source of 4.1 PgC yr⁻¹. For three broader zones, divided at 30°N and S, average fluxes that we deduce from 1980-1989 and 1990-1996 agree within about 1 PgC yr⁻¹ with decadal averages of 7 other inversion studies, except in the tropics where we find a larger source of CO₂ than most other studies in the 1980's and all other studies from 1990-1996. The interannual variability that we find exceeds that of most other studies.

PREFACE

This is the fourth of four articles that seeks to characterize sources and sinks of atmospheric CO₂ from direct measurements of the concentration and ¹³C/¹²C ratio. The articles, organized as though chapters of a single study, are referred to henceforth as Articles I to IV corresponding, respectively, to Keeling et al. [2001], Piper et al. [2001a,b], and Keeling and Piper [2001].

1. INTRODUCTION

In Articles I through III, measurements of atmospheric CO₂ at 9 stations in an array from the Arctic to the South Pole were used to deduce time-varying fluxes of the global carbon cycle. Article I presents an interpretation of these time-series data from 1978 through 1999 by an inverse procedure that identifies global reservoirs of carbon and fluxes of CO₂ exchanged between them. By a double deconvolution of the concentration and ¹³C/¹²C isotopic ratio of atmospheric CO₂, globally averaged at monthly intervals, and taking account of emissions of CO₂ from industrial activities, time-varying global exchange fluxes of atmospheric CO₂ with the terrestrial biosphere and oceans are deduced.

In Article II the same time-series data, but beginning in 1981, are used to resolve these global exchange fluxes into

polar, temperate and tropical constituents by means of an atmospheric transport model, TM2, whose surface boundary conditions are specified by source components that sum to the global fluxes of Article I. This inversion model adjusts a subset of these components until an optimal fit to the atmospheric observations is achieved. Then, consistent with these observations, it infers regional terrestrial biospheric and oceanic exchange fluxes assembled from these components for geographic zones divided at 23.5° and 47.0° in each hemisphere. The numerical stability of this inverse calculation is assured by specifying both temporal and spatial features of the components as far as *a priori* knowledge allows. In Article III a detailed analysis of model results is presented using sensitivity tests compared to a standard case, devised *a priori*. After comparing the results of these tests with the standard case, a preferred case was selected that is discussed further in this article.

Here, we first examine how well the inversion model, TM2, simulates the input atmospheric data. We then describe the regional fluxes inferred by inversion and consider the reliability of these estimates. We also make comparisons with other recent estimates of global and regional CO₂ exchange fluxes. We conclude by commenting on the significance of our results.

2. SIMULATION OF ATMOSPHERIC CO₂ DISTRIBUTION

2.1 Temporal variations

As described in Article II, with atmospheric transport model, TM2, we have simulated the distribution of atmospheric CO₂ concentration and ¹³C/¹²C ratio for a set of source components which define regional exchanges of atmospheric CO₂ with the land and the oceans and account for industrial CO₂ emissions. These components are identified with known processes, such as photosynthesis and respiration of land plants and air-sea gas exchange driven by changing CO₂ partial pressure differences at the ocean surface; their spatial and temporal variability are specified *a priori* from general knowledge of the global carbon cycle, but 4 terrestrial biospheric and 3 oceanic components for specified geographic zones are adjustable. By factors that determine their annual average flux, they are simultaneously set by a fitting procedure so that model TM2 predicts optimally both the observed annual average concentration and ¹³C/¹²C ratio of atmospheric CO₂ for each year of observations.

We have adopted the results of this inverse procedure for a preferred case [Article III, subsection 8.4, Figure 15a] that differs from a standard case [Article II, Figure 4] by setting

¹Scripps Institution of Oceanography, University of California, San Diego, California

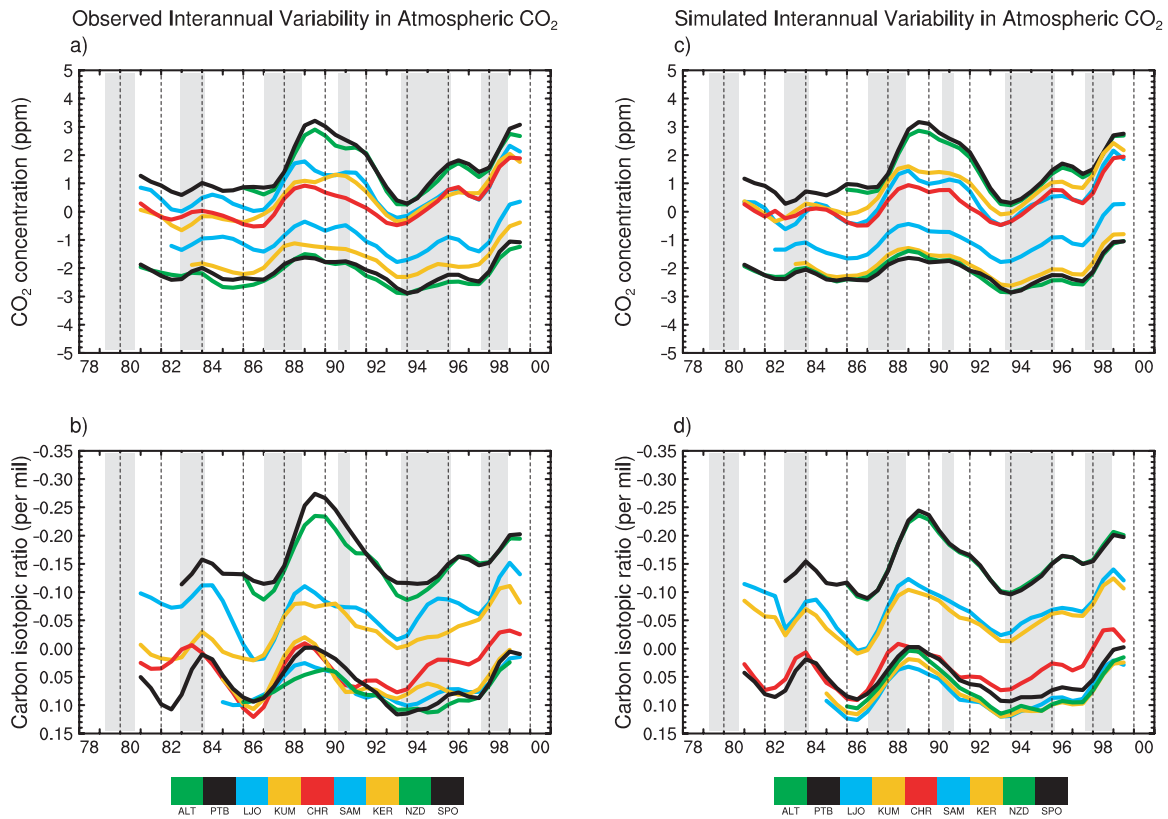


Fig. 1. Seasonally adjusted atmospheric CO_2 concentration, in ppm, and its $^{13}\text{C}/^{12}\text{C}$ reduced isotopic ratio, $\delta^{13}\text{C}$, in per mil, from 1981-1999, inclusive, from original measurements and as simulated by the inversion model. Linear trends, the same for all stations, have been subtracted for concentration and $\delta^{13}\text{C}$ as in Article I, Figure 4. Station code names, as shown on the color bar, are as defined in Article I, Table 1. Vertical gray bars demark approximately the times of El Niño events, inferred from time-intervals during which the rate of change of atmospheric CO_2 concentration at Mauna Loa Observatory, Hawaii, exceeded the trend in industrial CO_2 emissions, as shown in Figure 5 of Article I. **Panel a:** concentration data used as input to the model calculation. These data are the same as shown in Article I, Figure 4, except that the previously shown data, smoothed by a spline curve, have also been annually averaged at 6 month intervals. **Panel b:** same as Panel a, except for $\delta^{13}\text{C}$. **Panel c:** concentration data, the same as in Panel a, except as simulated by the inversion model. **Panel d:** same as Panel c, except for $\delta^{13}\text{C}$.

to zero the terrestrial fluxes of the 8° by 10° grid box of the observing station at La Jolla, California, without changing their global totals. In Figure 1, detrended annual averages of seasonally adjusted observations, and their simulations by the inversion model, are compared for all 9 stations. Concentrations are expressed as mole fractions in parts per million by volume (ppm) and the $^{13}\text{C}/^{12}\text{C}$ ratio by the reduced isotopic ratio, $\delta^{13}\text{C}$, in per mil (‰) relative to international standard PDB (see Article I, equation (1.1)). The plots are scaled vertically in the proportion, $\Delta\delta^{13}\text{C}/\Delta C = -0.050\text{ppm}^{-1}$, as in Article I (see equation (2.4)). Vertical gray bars demark times of rapid rise in the observed concentration of atmospheric CO_2 at Mauna Loa Observatory, Hawaii. These bars correlate with abnormally warm periods, spaced approximately four years apart, which are typically El Niño events (cf. Article I, Figure 5). The simulations show less variability and greater covariance for concentration and isotopic ratio than do the original data, but much of the original variability remains.

A closer examination of the difference between observations and simulations of atmospheric CO_2 is shown in Figure 2, after removing the average seasonal cycles of concentration and $\delta^{13}\text{C}$ for each observing station. Because amplitudes at all 9 stations have tended to increase over time, a linear gain in seasonal amplitude has also been removed, as

discussed in Article I. As shown by Figure 3 of Article I, seasonal cycles diminish from north to south. The scatter in the daily observations, plotted as dots, also diminishes from north to south, mainly as a result of interannual variability in seasonality, not removed in the seasonally adjusted data. The trends in the observations, shown by spline fits to the daily data (solid lines), are not fully realized by trends in the model simulations (dashed line segments), but patterns of variability are simulated almost as well as the scatter of the data justifies. The concentration and isotopic ratio clearly show similar patterns. (The isotopic data are plotted negative upward, scaled so that an increase in concentration of 1 ppm appears with the same interval on the plots as a decrease in $\delta^{13}\text{C}$ of 0.05 per mil, as in Figure 1.) Data and trends for a 10th station, Mauna Loa Observatory, Hawaii (Panel j), were not used in the inversion procedure (see Article II, section 5.)

2.2 Latitudinal gradients

As an additional test of the extent of agreement between atmospheric observations and model simulations, we show, in Figure 3, latitudinal profiles of concentration and $^{13}\text{C}/^{12}\text{C}$ ratio along a transect connecting the stations of our array (shown in Article I, Figure 1). Separate plots are shown,

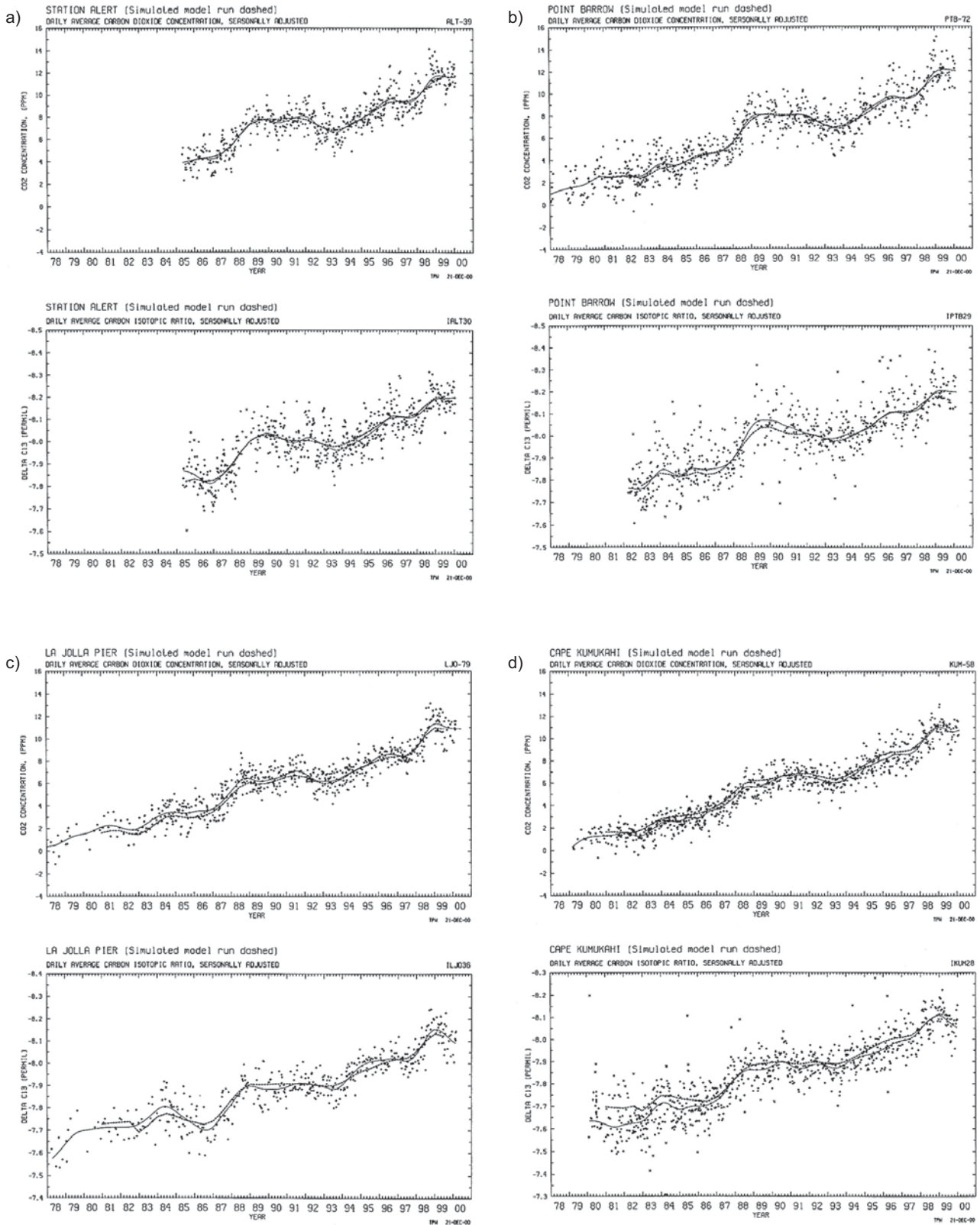


Fig. 2. Comparison of observed and simulated atmospheric CO₂ concentration, in ppm, and its reduced isotopic ratio, δ¹³C, in per mil, for 9 observing stations of our station array contributing to the inversion analysis (**Panels a through i**) and for Mauna Loa Observatory (**Panel j**). Seasonally adjusted daily average observations are shown as dots and as trends smoothed by spline curves (solid lines). Simulated data, at 6 month intervals, are shown as dashed line segments.

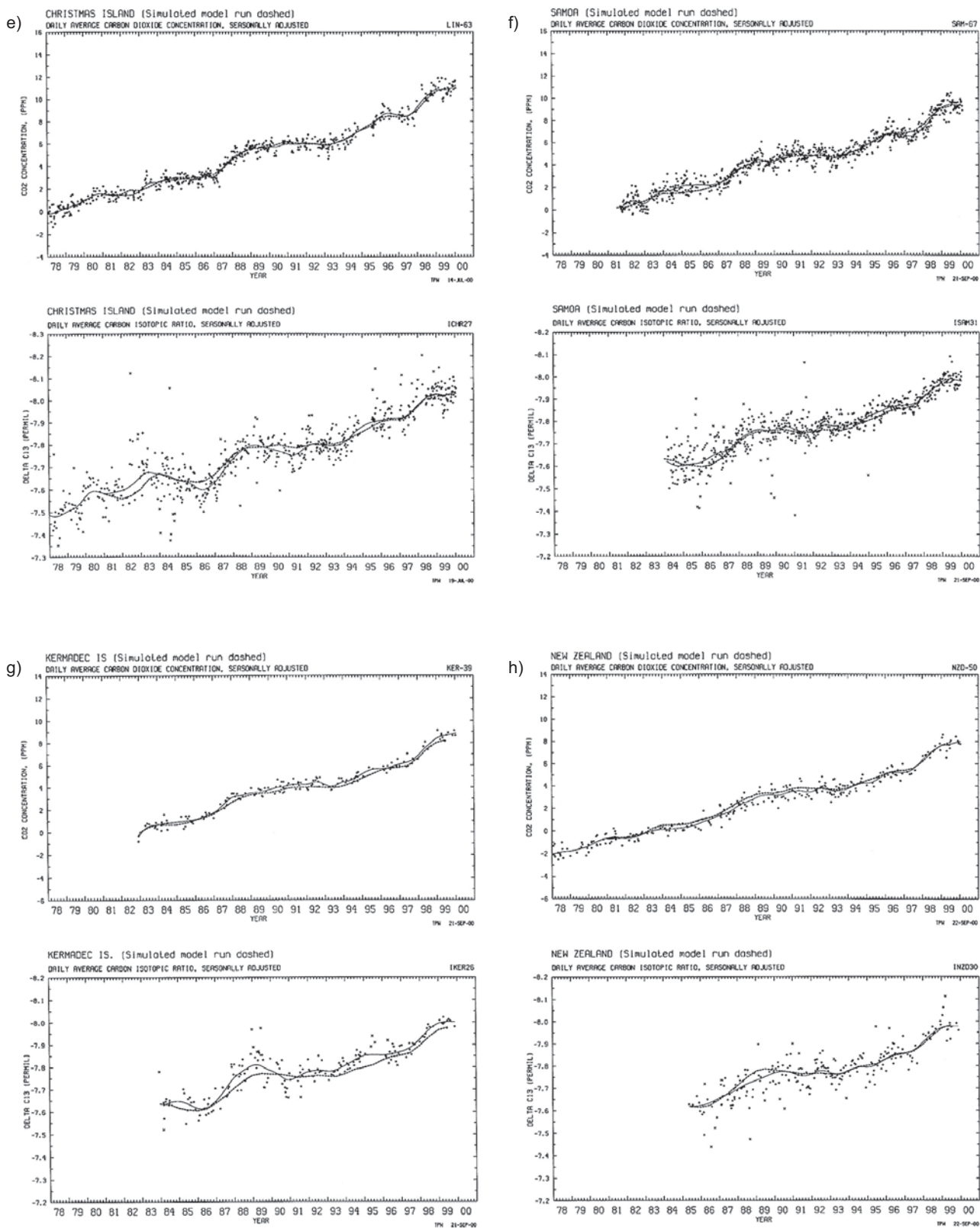


Fig. 2. Continued.

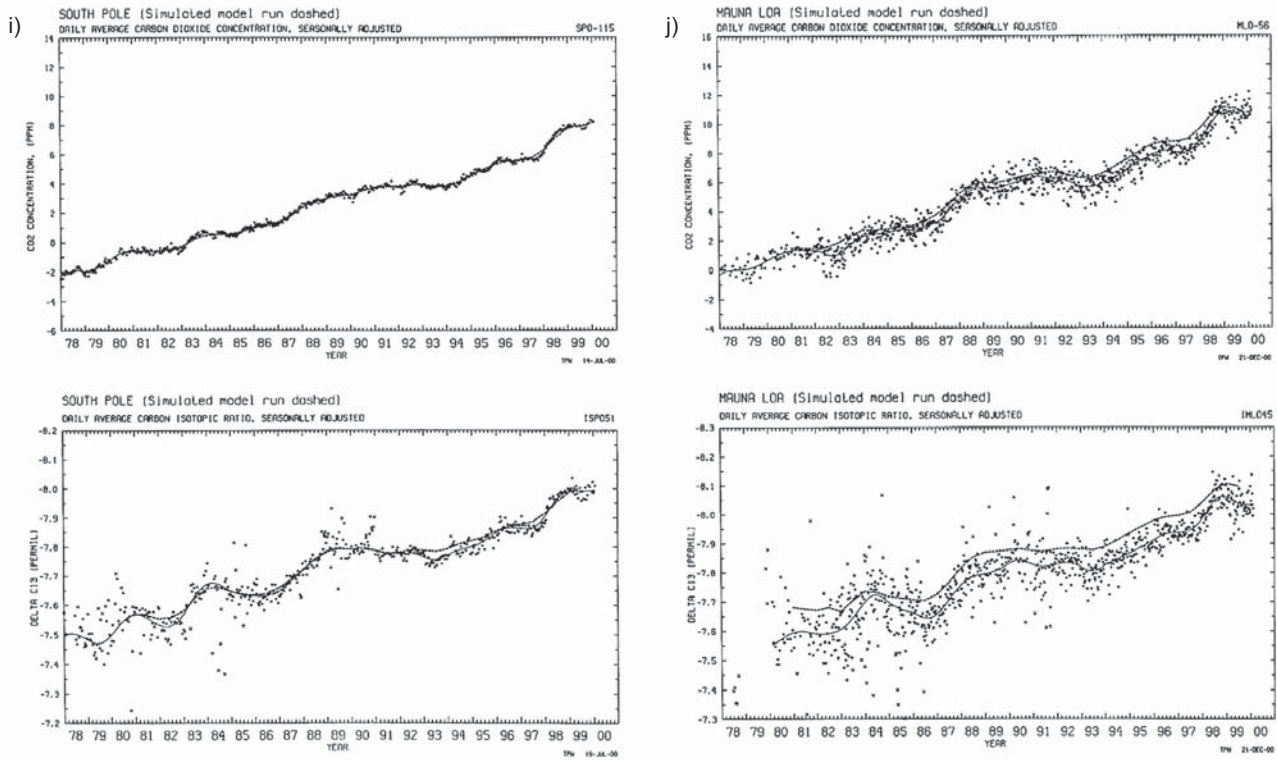


Fig. 2. Continued.

averaged for the 1980's, beginning in 1986, the first year in which we have complete isotopic records at all 9 stations, and also shown for the 1990's. The averaged station data (open circles) show strong latitudinal trends in concentration and $\delta^{13}\text{C}$ during both decades. The trend in concentration is almost steadily decreasing southward, but for $\delta^{13}\text{C}$ reverses near 45°S , a consequence of temperature-dependent isotopic fractionation of the oceanic exchange flux, that causes $\delta^{13}\text{C}$ to be more negative than otherwise at high latitudes relative to low latitudes [Keeling et al., 1989b, p. 323-4]. The dependency is not obvious in the northern hemisphere, because the imposed gradient mainly reinforces a gradient caused by other exchange flux constituents.

Error bars indicate twice the standard error of the data (2σ) with respect to the spline curve for each station, determined as described in Article I, Appendix D. The match of the simulations to the data fails to achieve the 2σ level, mostly because of persistent failure to simulate the observed gradients in midlatitudes of each hemisphere, especially between La Jolla and Cape Kumukahi in the northern hemisphere, and between Raoul Island, and New Zealand in the Southern Hemisphere. Except for the South Pole, all of the stations, although on seacoasts, are affected to some degree by the metabolic activity of land vegetation. Two stations, Baring Head and La Jolla, are also affected by nearby industrial CO_2 sources. By sampling during onshore winds, the effects of local sources are minimized, but contamination of background air doubtless contributes to the scatter seen in Figure 2.

The station at La Jolla, on the Pacific coast of California,

presents a difficult sampling problem, owing to its proximity to strong urban sources of industrial CO_2 and to more distant rural fluxes of CO_2 involving grasslands and forests. Because our research facility is at this site, we are able to select background air coming from the Pacific Ocean with a high degree of confidence that the air is not affected by continental fluxes directly from North America. However, the TM2 transport model that we use assumes industrial and biospheric fluxes to spread off shore almost a full grid box width (10°), because the La Jolla site is close to the eastern boundary of the box. As shown in Figure 4, the simulated gradient in atmospheric CO_2 is very strong at La Jolla, a deep CO_2 sink lying to the north and east of the station relative to CO_2 over the Pacific Ocean. This gradient is reflected in the aforementioned dips in the profiles of Figure 3 near 30°N . The deep sink reflects a strong uptake of CO_2 by the terrestrial biosphere, set by the model to reproduce as closely as possible the observations at La Jolla. The transport model, however, predicts only a slight gradient further west across the Pacific Ocean, where there are additional stations measuring CO_2 . Atmospheric CO_2 data for these other stations cannot be measured precisely enough to be a check on whether the gradient near La Jolla is more correctly simulated in the standard case or in our preferred case in which the gradient near La Jolla is reduced.

At other sampling locations, the CO_2 concentration profile is concordant with the observations almost within 2σ , in spite of the small error bars for several of these stations. Most significant is the good match for all three polar stations and for Christmas Island, near the equator, constraining the relative

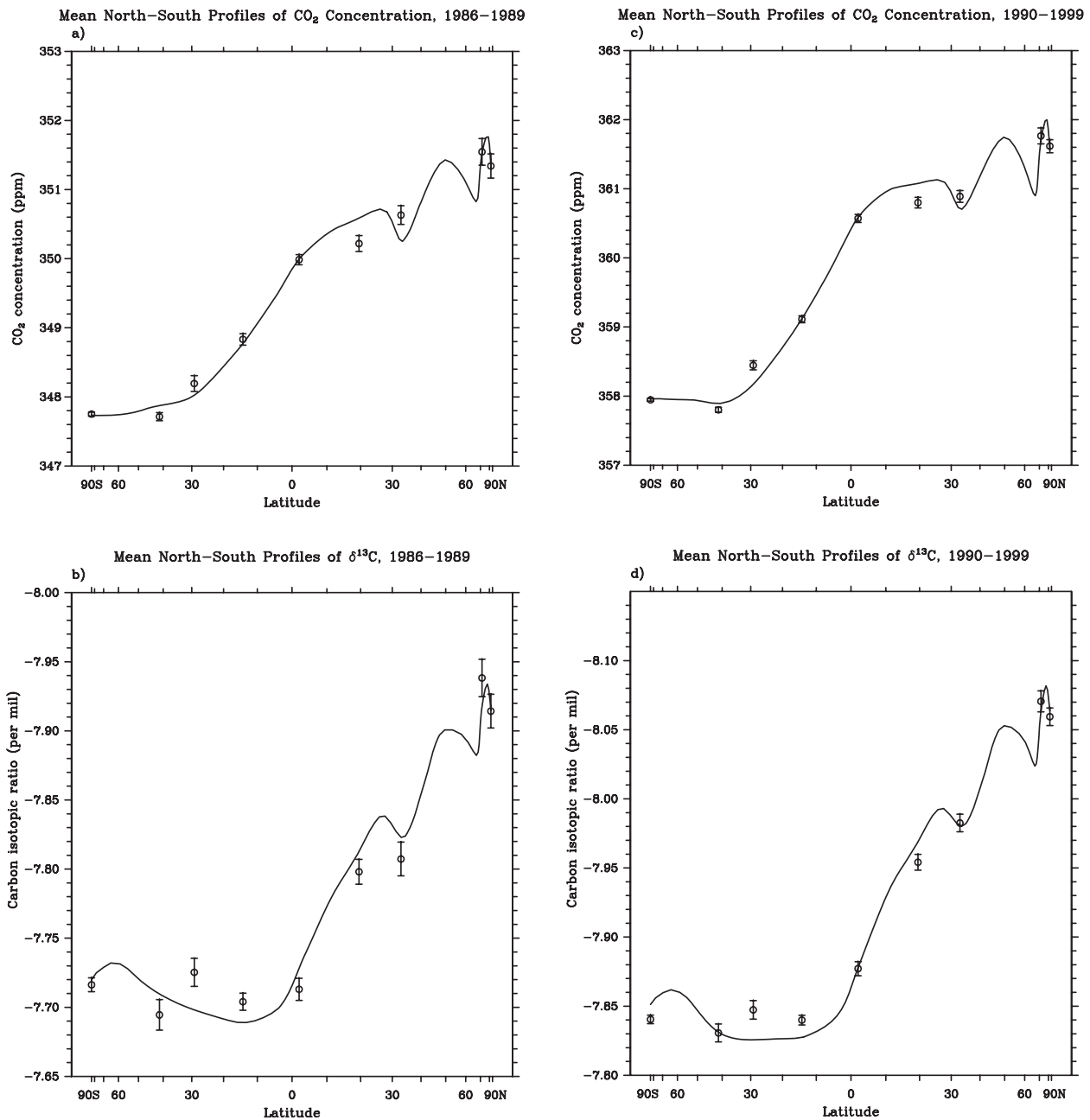


Fig. 3. North-south profiles of atmospheric CO_2 concentration, in ppm, and its reduced isotopic ratio, $\delta^{13}\text{C}$, in per mil, averaged from 1986 to 1989 and 1990 to 1999, inclusive. Observed mean values are shown by open circles. Bars indicate ± 2 standard errors of the estimated mean annual concentration for each station determined for each period averaged. Solid lines indicate values as simulated by the inversion model along a transect connecting the observing stations, as shown in Article I, Figure 2. The horizontal axis is scaled with respect to sine of latitude to be proportional to area on a sphere. **Panel a:** concentration for 1986 to 1989. **Panel b:** same, except for $\delta^{13}\text{C}$. **Panels c and d:** same as Panels a and b, respectively, except for 1990 to 1999.

strengths of the simulated tropical sources and sinks, compared to the extratropical.

3. SIMULATED REGIONAL FLUXES

3.1 Predicted terrestrial and oceanic carbon fluxes

The net annual atmospheric CO_2 exchange fluxes, derived by inversion in the preferred model simulation, are plotted in Figure 5 for the five climatic zones distinguished in this study. Terrestrial biospheric fluxes are shown in green, oceanic fluxes in blue. Also, in the lowest panel, are shown global fluxes derived by double deconvolution prior to making the regional

inversion calculations. The zonal fluxes shown in the five upper panels sum to these global fluxes by the fitting procedure of the inversion, as discussed in Article II, subsection 6.1. A black curve, in the bottom panel, represents a further sum of the separate global terrestrial and oceanic exchanges. Gray bars demark approximately the times of climatic events, typically El Niño events.

The most distinctive feature of the inferred fluxes shown in Figure 5 is a tendency of the terrestrial biosphere to have been a substantial net sink of atmospheric CO_2 in the northern temperate zone, but a substantial source in the tropics, where

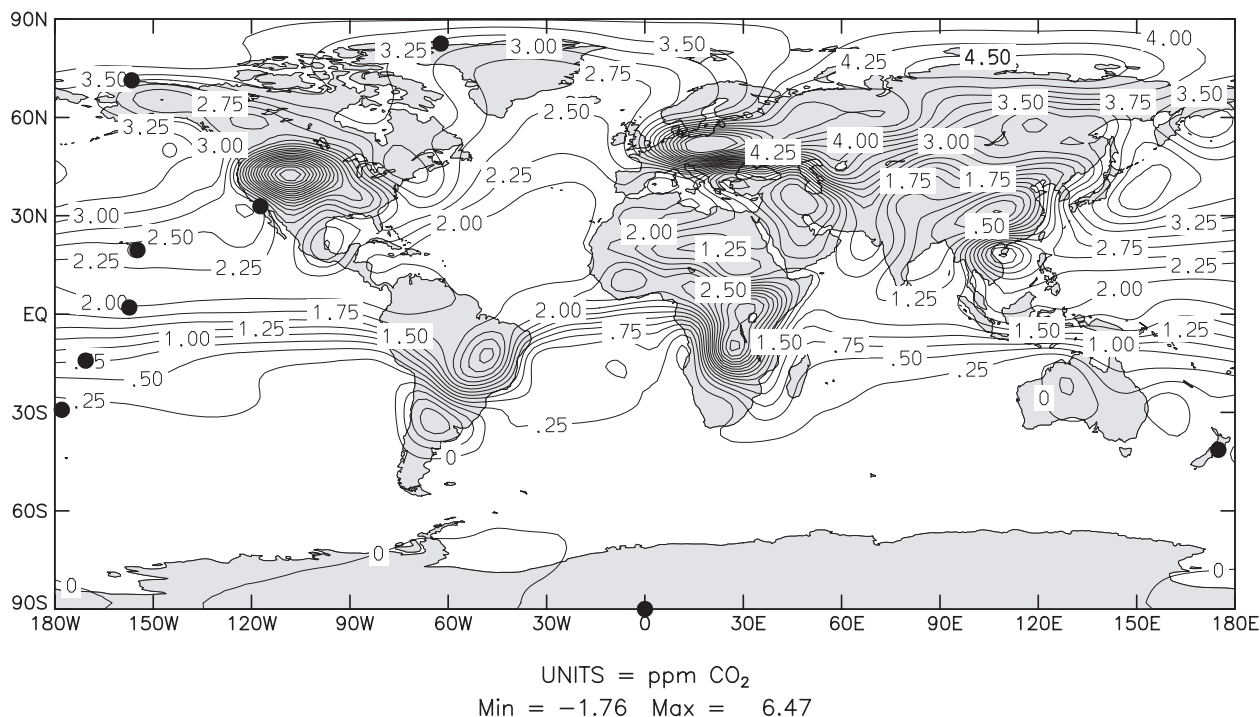
Mean Annual CO₂ Concentration Field at the Surface

Fig. 4. Contour map of the mean annual CO₂ concentration field, at the lowest model level, generated by the inversion model for the year 1986, chosen because the wind fields used in the transport model are for this year. Contour lines indicate concentration differences in ppm from that of the South Pole. Solid circles indicate locations of our station array, listed in Article I, Table 1.

it has varied over a wide range, especially in the 1990's, rising from near zero in 1990 to a peak of 6.7 PgC yr⁻¹ in 1998. A roughly similar pattern is seen in the global biospheric flux (bottom panel), reflecting the predominance of tropical flux in determining global variability.

In the northern polar zone, the terrestrial biospheric CO₂ flux rose irregularly to a peak in 1989 and afterwards generally declined. The peak reflects unusually high CO₂ concentrations and negative ¹³C/¹²C ratios in 1989 at the Point Barrow and Alert stations (see Figure 4 of Article I), and also relates to an unusually strong polar seasonal cycle [Keeling et al., 1996]. As discussed in subsection 5.5, below, both plant growth and respiration appear to have been anomalously high in the late 1980's but the latter more than the former. The terrestrial biosphere became a distinct sink of atmospheric CO₂ in the northern hemisphere during the mid-1980's, in the southern hemisphere during the 1990's.

The inferred oceanic CO₂ fluxes varied considerably less than the terrestrial fluxes. They varied most in the tropics during the 1980's, anticorrelated with the terrestrial biospheric fluxes on the time-scale of prominent recurring abnormally warm periods (cf. gray bars in Figure 5) which we will henceforth call the "El Niño time-scale." As was the case for the terrestrial biosphere, the pattern of oceanic variations in the tropics is similar to its global average, but with a lesser range of variability.

3.2 Evaluation of zonal fluxes found by inversion

The findings described above suggest large temporal variability in the sources and sinks of atmospheric CO₂. We now consider the trustworthiness of these findings.

The combined global biospheric and oceanic sink, derived directly from the global average CO₂ concentration data, as discussed in Article I, is well established; its computation depends only on a precisely determined, globally averaged atmospheric CO₂ concentration and a slowly varying release of CO₂ from industrial sources, computed from a well-defined data base of fossil fuel production and cement manufacture. This combined sink, on annual average, has fluctuated by 3.6 PgC yr⁻¹ since 1978, as shown by the black curve in the bottom panel of Figure 5. The fluctuations closely correlate with climatic events (seen in relation to the gray bars). The magnitude of these fluctuations is not in doubt.

Less certain, because the calculations assume that the ¹³C/¹²C isotopic discrimination of photosynthesis on land has not varied interannually, are inferred variations in the separate global terrestrial and oceanic fluxes, also shown in the bottom panel. If the assumption of constant discrimination is correct, variations in the terrestrial flux are so large, a range of over 7 PgC yr⁻¹, as to require substantial variations in the global oceanic flux, nearly opposite in phase. However, the fluxes for temperate and polar zones seen in Figure 5 do not show opposing terrestrial and oceanic global patterns that would suggest variable extratropical discrimination. Errors in our calculations, because we neglect to consider variable

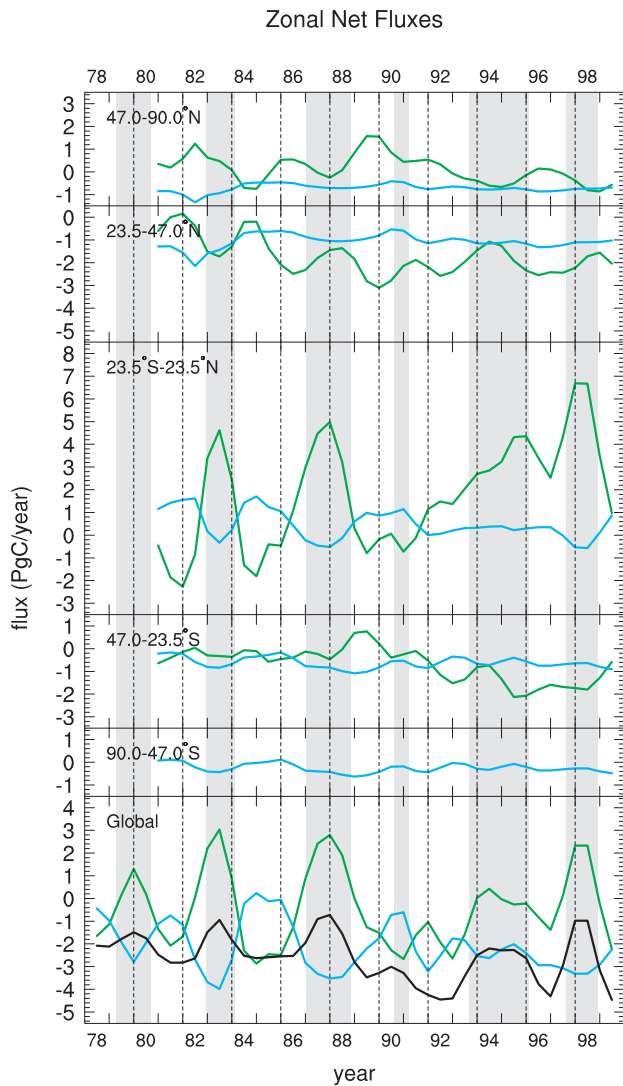


Fig. 5. Net annual CO_2 exchange fluxes, in PgC yr^{-1} versus time, positive to the atmosphere, as generated by our inversion model in a preferred calculation (see text, subsection 2.2). Fluxes are shown for the terrestrial biosphere (green) and the oceans (blue) for 5 latitudinal zones, at 6 month intervals. Corresponding global fluxes, and their sum (black curve), are shown in the bottom panel. Vertical gray bars are as in Figure 1.

discrimination, evidently should apply mainly to the tropics, as noted in Article II, section 8.

The sensitivity of inferred CO_2 fluxes to interannual variability in our $^{13}\text{C}/^{12}\text{C}$ data is tested by an alternate calculation, shown in Figure 6, in which isotopic data contribute to the calculation only to set the average magnitudes of the 3 adjustable oceanic source components to be the same as in the calculation shown in Figure 5. (This sensitivity test is the same as that shown in Article III, Figure 17, except that, as a reference, the preferred case is substituted for the standard case). With temporal variability in the $^{13}\text{C}/^{12}\text{C}$ data ignored, the terrestrial biospheric fluxes outside of the tropics show little change from the preferred case of Figure 5. In contrast, in the tropics the biospheric flux shows sharply reduced fluctuations, especially in association with three strong El Niño events in 1983, 1987, and 1998. Thus, the zonal fluxes calculated by our standard inverse procedure depend on our

isotopic data mainly to establish average strengths in all zones, and to infer large tropical fluctuations associated with strong El Niño events. As discussed in Article III, subsection 8.6, the closely matched phasing of global signals of the $^{13}\text{C}/^{12}\text{C}$ and concentration of atmospheric CO_2 (seen in Article I, Figure 7) makes probable that globally significant changes in isotopic discrimination occur mainly in phase with strong El Niño events and other abnormally warm episodes that occur predominantly in the tropics.

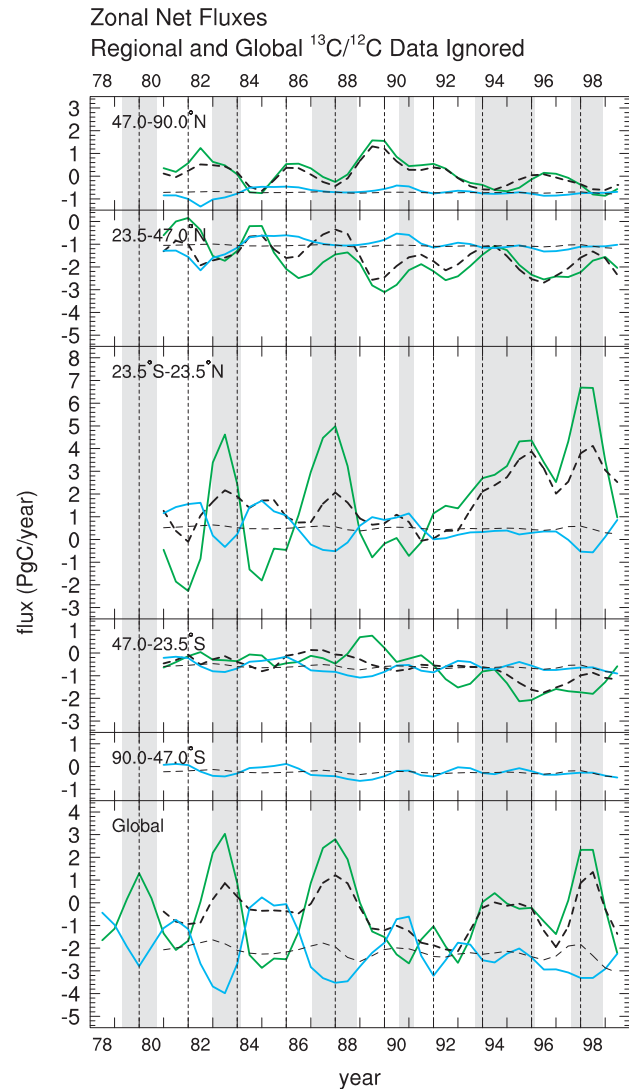


Fig. 6. Comparison of the model simulation of Figure 5, (thin green and blue lines) with a model simulation (black dashed lines) in which isotopic data are used only to establish average fluxes for each zone, as explained in the text. Thick dashed lines indicate terrestrial biospheric fluxes, thin dashed lines indicate oceanic fluxes in all panels.

4. COMPARISON WITH OTHER STUDIES

4.1 Introduction

Our inversion-based calculation of sources and sinks of atmospheric CO_2 , by spanning nearly two decades, reveals both short-term variability in the carbon cycle, presumably of mostly natural origin, as discussed in the previous subsection, and also longer term variability that may involve significant

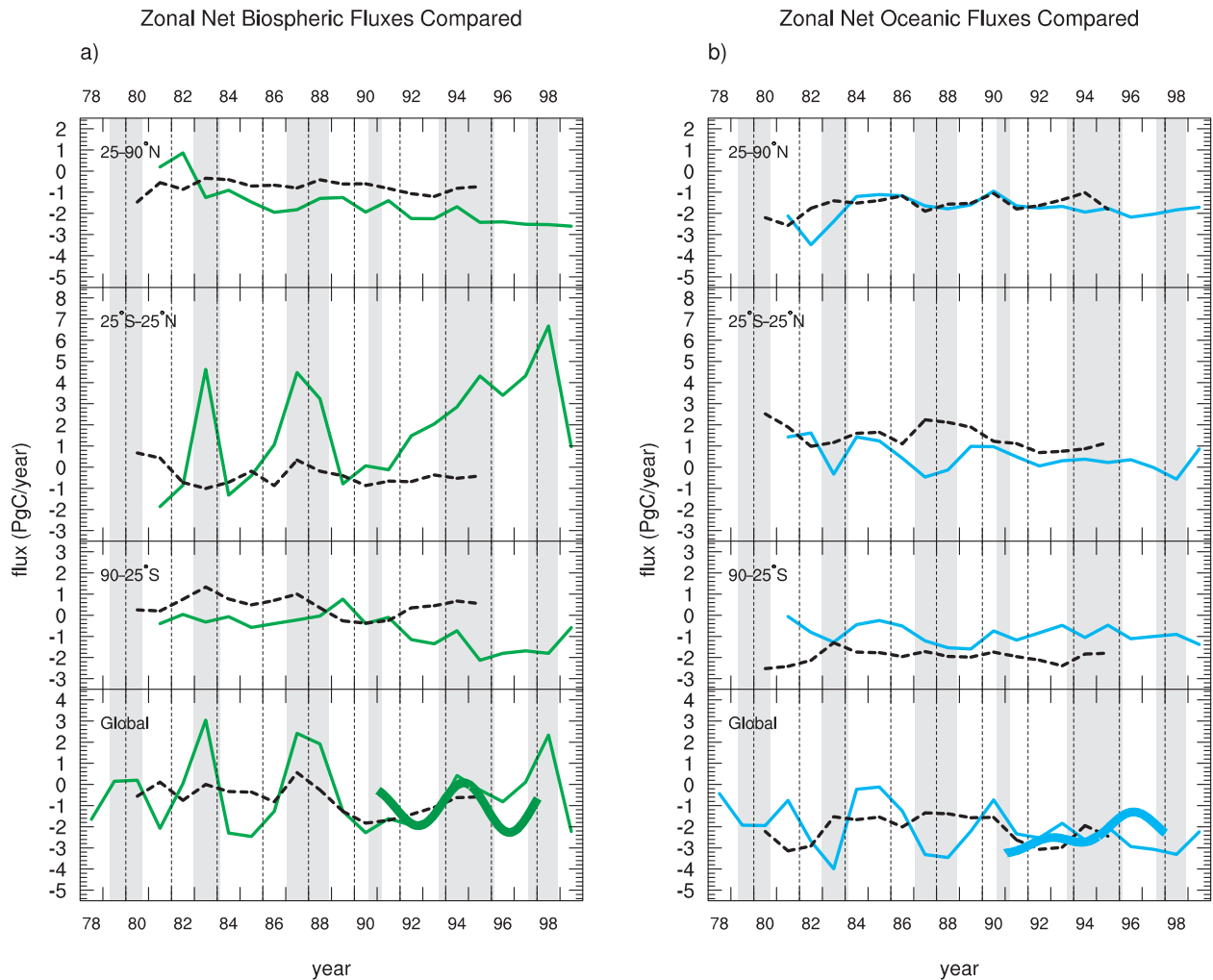


Fig. 7. Comparison of net annual CO_2 exchange fluxes generated by our inversion model (solid lines), as in Figure 5, but with zonal fluxes regridded and compared with simulations by Rayner et al. [1999a] (dashed lines). **Panel a:** Terrestrial biospheric fluxes. **Panel b:** Oceanic fluxes. Also shown, in the bottom panels, are simulated global fluxes by Battle et al. [2000] (thick green curve in Panel a, thick blue curve in Panel b). Vertical gray bars as in Figure 1.

responses to human activities. But these findings must be substantially correct to contribute to a better understanding of the carbon cycle, a difficult goal to achieve, because of the complexity of the carbon cycle. As noted in Article I, many more data are available than we have used in our study, including an extensive dataset compiled by the Climate Monitoring and Diagnostics Laboratory of the United States National Oceanic and Atmospheric Administration (CMDL/NOAA) [Conway et al., 1994; Masarie and Tans, 1995]. We have postponed merging our data with other data until better cross-calibration can be achieved. Also we prefer initially to use concentration and $^{13}\text{C}/^{12}\text{C}$ ratio data derived from the same air samples, and analyzed using nearly unchanging protocols.

To put our findings into perspective, we now present comparisons with other studies. These include two recent inversion studies that present time-series results that can be compared with our study, and several studies that use process-based terrestrial biospheric models, driven by climatic and biological data, to predict terrestrial biospheric fluxes over extended periods. Predictions of these process models test the possible range and likely phasing of variability in biological fluxes and

how temperature and precipitation may drive this variability. We also compare our findings with 7 inversion studies at coarse scales in space and time.

4.2 Temporal variability

The longest regionally resolved inversion calculation comparable to ours that utilizes both concentration and $^{13}\text{C}/^{12}\text{C}$ data of atmospheric CO_2 is by Rayner et al. [1999a, Figure 7]. In our Figure 7 is shown their plots of terrestrial biospheric and oceanic fluxes for three latitude bands, divided at 25°N and S , together with plots of our corresponding fluxes, interpolated to their meridional grid spacing. On a global scale the two sets of plots show some correspondence, but regionally neither the short-term variability nor the long-term averaged fluxes of the two studies agree. An earlier study [Francey et al., 1995], shown by Rayner et al. [1999a, Figure 6], using nearly the same data produced somewhat different annual global averages, but no better agreement with our results. On the other hand, when the data quoted in these studies were used to infer the sum of the biospheric and oceanic fluxes from 15°S to 30°N [Rayner et al., 1999b], they obtain similar

results to ours, as shown in Figure 8, for the case, shown in Figure 6, where we ignored interannual variability in our $^{13}\text{C}/^{12}\text{C}$ data. The discrepancies between these studies, as seen in Figure 7, therefore, are owing mainly to their isotopic data showing far less interannual variability than our data. It has not been resolved whether their isotopic data from Cape Grim, Tasmania or ours are more nearly correct.

Zonal Net Biospheric + Oceanic Fluxes Compared

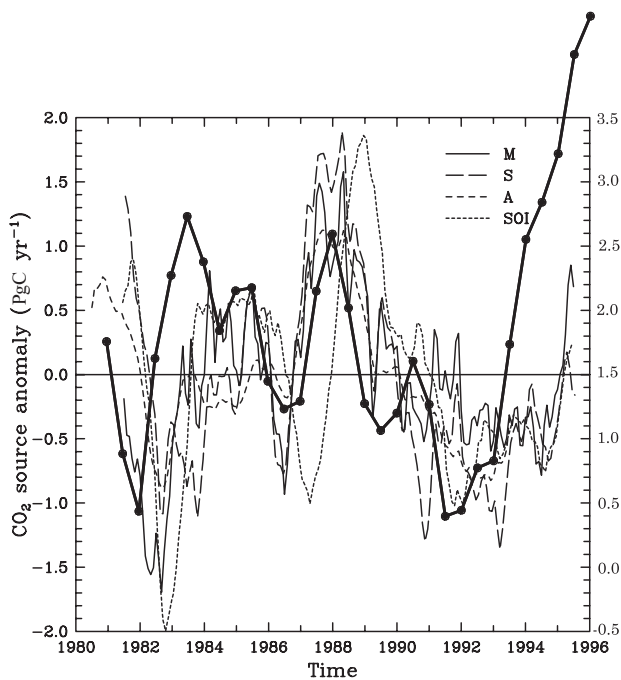


Fig. 8. Net annual CO_2 exchange fluxes, in PgC yr^{-1} (left vertical axis label), positive to the atmosphere, simulated by three inversion models (solid lines and long and medium dashed lines) from 1980 to 1995 adapted from Rayner et al. [1999b, Figure 1]. The fluxes represent the sum of terrestrial biospheric and oceanic fluxes averaged between 15°S and 30°N . Also adapted from Rayner et al. [loc. cit.] is a plot of the southern oscillation index, (short dashed line, no scale indicated). Our determination of net annual CO_2 exchange from 23.5°S to 23.5°N is shown for comparison (solid circles connected at 6-month intervals, by a heavy black line). This plot is derived from the sum of the terrestrial biospheric and oceanic fluxes shown in the third panel of Figure 6.

The $^{13}\text{C}/^{12}\text{C}$ record at Cape Grim is the only isotopic record that we know of, besides ours, that spans most of the 1980's. Beginning in 1991, however, data from a large array of stations contributing to the CMDL/NOAA dataset [Troler et al., 1996] provide an additional comparison. The global terrestrial biospheric flux inferred using these data [Battle et al., 2000], plotted in Figure 7, Panel a, shows substantial agreement with our corresponding flux, taking into account that the plot is a two-year averaged trend, and that the first and last years, as plotted, are only partially based on contemporary data, because of an assumption that the data of the first and last observing years are "representative" of the preceding and succeeding years, respectively (see their note 28.). In the perspective of the general agreement between global biospheric flux of our study and this latter study, the global corresponding flux found by Rayner et al. [1999a],

appears to be heavily smoothed. The oceanic flux of Battle et al. [2000] shows fair agreement with our results (see Figure 7, Panel b).

An additional resource for probing the extent of interannual variability in terrestrial biospheric fluxes are predictions from process-based terrestrial biospheric models (TBM's). In Figure 9, the predictions of 4 such models, reported by McGuire et al. [2001], are compared with our inferred biospheric fluxes of Figure 5, interpolated into zones, divided at 30°N and S and at 45°N , and from 30° to 50°S in a south temperate zone. In the mainly-extratropical zones, variability in the four TBM predictions shows little mutual consistency, or consistency with the variability seen in our fluxes. In the mainly-tropical zone, 30°N - 30°S , however, all five predictions correlate at times of peak releases of CO_2 related to El Niño events. This pattern is also reflected in global averages, shown in the bottom panel of Figure 9. The amplitudes of these tropical and global fluctuations, however, differ considerably for different TBM's, and most amplitudes are less than we find.

The fluxes predicted by the TBM's that show the greatest variability, IBIS and LPJ, are replotted in Figure 10 for better visualization. In the tropics these fluxes show considerable similarity with our inferred fluxes and show some similarity in the other zones. The TBM fluxes when averaged for the broader zone from 30° to 90°N (not plotted here), agree still better. From these comparisons we judge that the large temporal variability in terrestrial biospheric fluxes that we infer by inversion finds some support in predictions by TBM's over broad zones, but that persistent sources and sinks for the narrower zones of our inversion study are not confirmed.

As a final comparison of predicted temporal variability, we consider terrestrial biospheric fluxes just for the United States of America. In Figure 11 is shown the average of predictions of 3 TBM's: Biome-BGC, Century, and TEM, carried out in a coordinated study, the Vegetation/Ecosystem Modeling and Analysis Project (VEMAP), using almost identical databases for model input data [Schimel et al., 2000]. Our calculated flux, as shown, is simply prorated in strength to the fraction of net primary production of land vegetation that we calculate for the coterminous United States compared with that of the entire latitude band. The variability of the VEMAP fluxes is less than half of what we find, but the pattern is similar, suggesting that the factors that drive these 3 TBM's are to some extent reflected in our flux. As with the four previously discussed TBM's, there is very little evidence of any persistent net flux, whereas, just for the United States alone, we find a sink of about 0.6 PgC yr^{-1} .

4.3 Regional variability

The geographic distribution of sources and sinks of the carbon cycle has been reported in a considerable number of studies using inverse modeling of atmospheric transport. There is a recent comparison of outputs from 8 such studies, including ours, supplied by participants of the TRANSCOM project, an initiative of the Global Analysis Integration and Modeling (GAIM) task force of the International Geosphere Biosphere Program (IGBP). Comparisons were made of averaged source

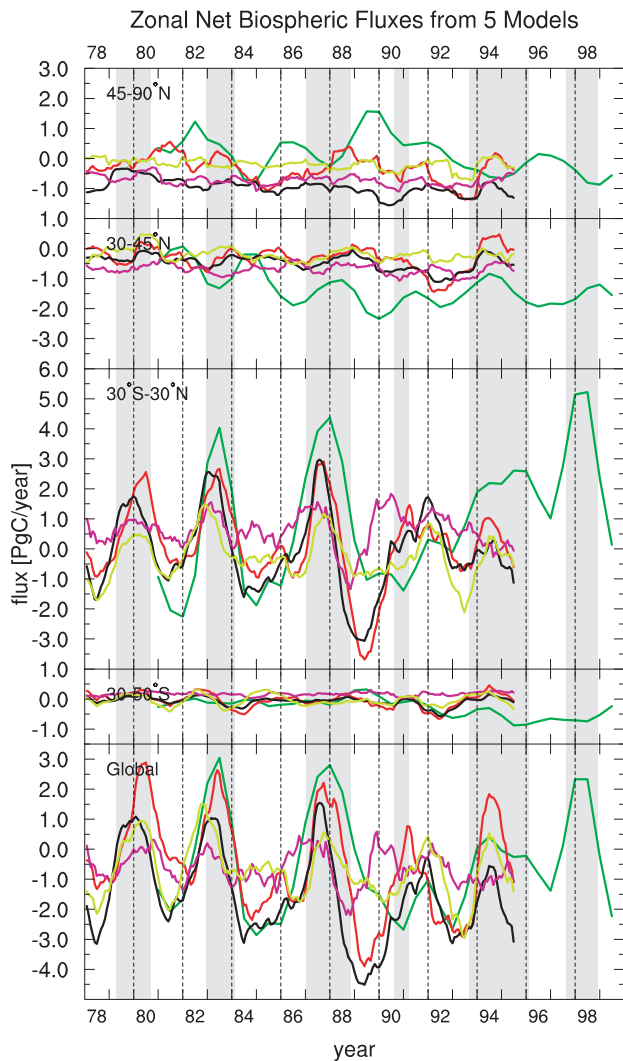


Fig. 9. Net annual CO₂ exchange fluxes, in PgC yr⁻¹, positive to the atmosphere, for the terrestrial biosphere, simulated by 4 process-based terrestrial biospheric models as reported by McGuire et al. [2001]. Data are shown for HRBM model (purple), IBIS model (black), LPJ model (red) and TEM model (light green). The models are described in the referenced article. For comparison, the inferred fluxes of Figure 5 generated by our inversion model are also shown (dark green curves), regridded to 4 latitudinal bands, as labeled. Vertical gray bars are as in Figure 1.

strengths, separated into terrestrial biospheric and oceanic, over coarse spatial and temporal domains: 3 geographic zones (in this study called "latitude bands") divided at 30°N and S and two decadal, or nearly decadal, time periods, 1980-89, and 1990-96, inclusive [Heimann, 2000].

In Table 1 is listed the results from our preferred case, and, in Figure 12, plots of the results of all of the studies (the others anonymous). To accommodate the grid spacing of our model, and the periods of our data sets, we modified the spatial and temporal domains of the TRANSCOM project slightly, using zonal separations at 31.3°N and S and reducing the first period of averaging to begin in July, 1981. Because our study extends through the 1990's, we also include averages in Table 1 for the whole decade.

We first note that all of the studies, except one, agree closely on the meridional partitioning of the combined oceanic

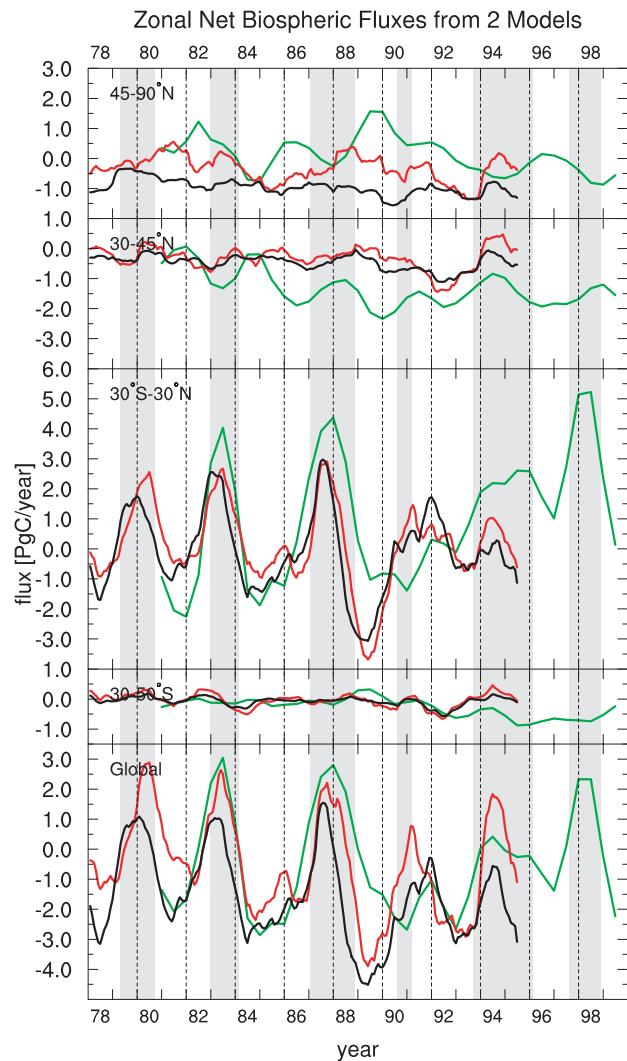


Fig. 10. Same as Figure 9, but only for comparisons with the IBIS and LPJ models.

and terrestrial biospheric fluxes poleward of 30°N and S (shown in light blue) for both 1980-1989 and 1990-1996. The partitioning with respect to ocean and land, however, and the combined flux in the 30°N to 30°S band, show considerably poorer agreement.

For the northern band, 30°N to 90°N, we infer from our model results only a moderate terrestrial biospheric sink, produced by merging the large temperate terrestrial biospheric sink between 30°N and 47°N that we find with a small source north of 47° (see Figure 5). For the 1980's, all other studies but one infer a larger biospheric sink than our study does, but, for the 1990's, we compute a larger sink, exceeding that of all but two other studies. For the 1980's, our oceanic sink is the largest reported, though in close agreement with three other studies. For the 1990's, our sink exceeds that of all but one other study.

For the tropical band, we compute a biospheric source of about 0.5 PgC yr⁻¹ in the 1980's, exceeded by only two other studies, and about 1.0 PgC yr⁻¹ in the 1990's, exceeded by none. Indeed, most studies report a biospheric sink in the 1990's, as great as -1.3 PgC yr⁻¹. We find very weak oceanic

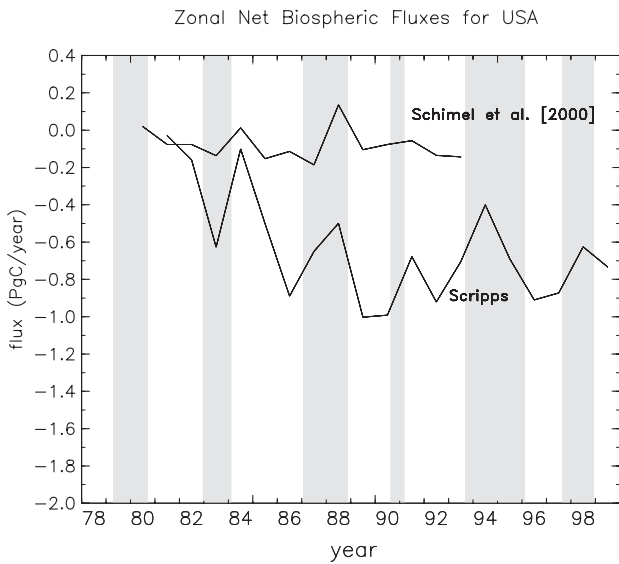


Fig. 11. Net annual CO₂ exchange fluxes, in PgC yr⁻¹, positive to the atmosphere, for the terrestrial biosphere, for the coterminous United States of America. The upper curve shows the average of simulations by 3 terrestrial biosphere models, as reported by Schimel et al. [2000]. The lower curve shows a corresponding flux simulated by our inversion model for the temperate zone, prorated to refer only to the United States, as described in the text. Gray bars are as in Figure 5.

Exchange Fluxes from 8 Inversion Studies

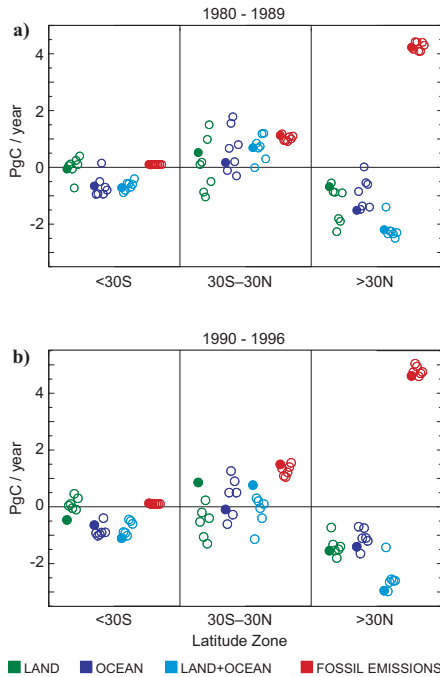


Fig. 12. Average net annual CO₂ exchanges for three latitudinal bands, as labeled, in PgC yr⁻¹, found in independent inversion studies, as reported by Heimann [2000]. There are 8 studies for the 1980's, 7 studies for the 1990's (1990-1996). Our findings are shown by solid circles, others by open circles. Color coding distinguishes terrestrial biospheric (land) and oceanic fluxes, their sum, and fossil emissions. **Panel a:** averages from 1980 to 1989, inclusive (shorter time period for some studies). **Panel b:** same except for 1990 to 1996, inclusive.

TABLE 1
ESTIMATES OF SOURCES AND SINKS, IN PgC YR⁻¹, FOR 3 LATITUDE BANDS^a

1981-1989					
	bio	oce	bio+oce	foss	atm
31.3-90N	-0.683	-1.512	-2.195	4.229	
31.3S-31.3N	0.522	0.171	0.692	1.129	
31.3-90S	-0.057	-0.659	-0.716	0.104	
Global	-0.218	-2.000	-2.218	5.462	3.243
1990-1996					
	bio	oce	bio+oce	foss	atm
31.3-90N	-1.547	-1.405	-2.952	4.610	
31.3S-31.3N	0.857	-0.094	0.764	1.493	
31.3-90S	-0.463	-0.644	-1.107	0.125	
Global	-1.152	-2.142	-3.294	6.228	2.934
1990-1999					
	bio	oce	bio+oce	foss	atm
31.3-90N	-1.700	-1.444	-3.144	4.703	
31.3S-31.3N	1.409	-0.204	1.205	1.581	
31.3-90S	-0.496	-0.712	-1.208	0.130	
Global	-0.786	-2.361	-3.147	6.414	3.266
1981-1999					
	bio	oce	bio+oce	foss	atm
31.3-90N	-1.218	-1.476	-2.694	4.479	
31.3S-31.3N	0.989	-0.027	0.962	1.367	
31.3-90S	-0.288	-0.687	-0.975	0.117	
Global	-0.517	-2.190	-2.707	5.963	3.255

^a Fluxes to the atmosphere are positive numbers. bio = terrestrial biospheric reservoir, oce = ocean reservoir, foss = CO₂ from fossil fuel combustion and cement manufacture, atm = rate of increase of atmospheric CO₂.

net fluxes in both decades, whereas four of the other studies report moderately strong sources.

For the southern band, we find a very small biospheric sink in the 1980's, increasing to -0.5 PgC yr⁻¹ in the 1990's, whereas all of the other studies, except one in the 1980's, report a smaller sink, or a weak source in the 1990's. All studies, including ours, report a moderate oceanic sink for both decades, except for the single study in the 1980's.

In summary, the overall agreement among the studies compared by Heimann [2000] with respect to the biospheric and oceanic partitioning of CO₂ fluxes is insufficient to assess clearly the degree of agreement of our study with the other studies individually. Our calculated fluxes conform to the norm of the other studies except for the mainly tropical band, where even the sum of the terrestrial and oceanic fluxes, averaged from 1990-1996, agrees poorly among the individual studies. On a more optimistic note, the best general agreement is for the northern band, where a preponderance of the global emission of CO₂ from fossil fuel is emitted by industrial nations. Given the recent concern about mitigating these emissions [Framework Convention on Climate Change, 1997] it is reassuring that the inversion studies compared here, including ours, generally agree for this latitude band.

5. DISCUSSION

5.1 Introduction

Several issues are raised by the character of the temporal and meridional variability in carbon cycle fluxes that we deduce from our records of the concentration and $^{13}\text{C}/^{12}\text{C}$ ratio of atmospheric CO_2 . Are the data that we use reliable? Is the inverse procedure that we use to interpret our measurements realistic? Even if we cannot fully answer these questions, can we judge the worth of our findings by how they compare with other studies of carbon cycle fluxes? How do our findings contribute to an understanding of the carbon cycle?

5.2 Considerations of input atmospheric data

We have maintained essentially the same procedures for measuring the concentration of CO_2 throughout this study, as described by Keeling et al. [1989a] and in Appendices A and B of Article I. Our isotopic measurements, however, have changed over time. The laboratory performing mass-spectrometric analysis changed from Groningen University in the Netherlands to the Scripps Institution of Oceanography (SIO) near the beginning of 1991, as discussed in Article I, Appendix C. From plots (Article I, Figure 3) it is apparent that the scatter in our isotopic data decreased immediately after the change of laboratories. Because sampling errors, determined from replicate samples, did not change significantly, the reduced scatter is evidently owing to better calibration and spectrometer performance after 1990. Also, after the change in laboratories, we found and corrected for a differential drift in isotopic calibration by comparing standards of CO_2 gas extracted from natural air, containing nitrous oxide, with standards of pure CO_2 . We have no knowledge whether a similar drift problem may have existed at Groningen University in the 1980's since at that time none of the standards in use contained atmospheric N_2 . Also the isotopic data during the final years of Groningen analyses, 1989-1991, were less reliably calibrated than earlier, as noted in Article I. It is quite evident that the reliability of our isotopic data improved after 1990.

In spite of this improvement, the magnitude of interannual fluctuations in our isotopic data is similar for the 1980's and 1990's, as seen in our records for individual stations (Article I, Figures 3 and 4), and more decisively in the rate of change of their global average (Article I, Figure 7), which is attributed to variability in the global average net terrestrial biospheric flux (Article I, Figure 9b). Furthermore, calibrations applied to analyses at Groningen University have been reviewed with no evidence that errors before 1989 caused the large fluctuations seen in the data associated with the El Niño events of 1982-3 and 1987-8 [Harro Meijer, private communication]. Therefore we regard these data as probably reliable and believe that, if variations in inferred tropical flux are exaggerated, the cause stems from some defect in our model formulation.

5.3 Modeling considerations

Our adopted model source components are based mainly on generally accepted criteria applied to processes such as air-sea exchange of CO_2 , vertical mixing in the oceans (albeit highly

simplified), photosynthesis and heterotrophic respiration of land plants and soils, and to fossil fuel combustion. Our computations of CO_2 exchange fluxes depend also, however, on two less well established procedures: scaling of remotely sensed vegetative index (NDVI) data to determine net primary production of land plants and estimates of terrestrial biological exchange fluxes from land disturbances and land use changes. Indeed, zonal averages of these fluxes were adjusted in our inversion analysis to conform to our atmospheric data. Also, as discussed in Article I, the double deconvolution procedure using atmospheric $^{13}\text{C}/^{12}\text{C}$ data does not establish the long term average partitioning of sources and sinks of atmospheric CO_2 between terrestrial and oceanic. In Article I we show that our estimates of global partitioning are close to those adopted by the Second Assessment Report of the IPCC [Houghton et al., 1996], but our study offers no assurance that these estimates are correct.

Furthermore, unresolved is the extent to which our model produces errors in inferred terrestrial biological fluxes because we have assumed that isotopic discrimination against the rare isotope, ^{13}C , by plants is constant in time. Variations in discrimination as small as 1‰, such as we see in the diurnal and seasonal cycles of atmospheric CO_2 at single sites, if they occur synchronously over large regions, could alter our inferred biological fluxes significantly, as pointed out in Article I, section 5. The remarkable covariance of concentration and $^{13}\text{C}/^{12}\text{C}$ ratio in our data over nearly two decades, however, makes likely that the only significant wide-spread temporal variations in discrimination in these data are responses to the same processes that cause changes in CO_2 concentration associated with the El Niño cycle.

After finding large fluctuations in terrestrial biospheric fluxes in the 1980's we hoped that the next important El Niño event would help establish whether such fluctuations were typical of the El Niño cycle, or were possibly artifacts. Our data for the 1998 event clearly show a repetition of the strong covariance found in the 1980's and a similar range of variation in our $^{13}\text{C}/^{12}\text{C}$ signal, but the range of variation in the concentration signal is substantially greater, so that the double deconvolution indicated a lesser opposing oceanic signal than for the 1980's (Article I, Figure 10c and 10d). This opposing signal, so pronounced in our computed oceanic flux for the 1980's, could be construed to be the inevitable consequence of isotopic data falsely showing too large a terrestrial signal [Francey et al., 1995], but this explanation is less likely to apply to the 1998 event, because our isotopic data were then better calibrated, as pointed out in subsection 5.2. If isotopic discrimination explains part of our $^{13}\text{C}/^{12}\text{C}$ signal, was it more pronounced for the events of the 1980s or was it similar in both decades, the oceanic signals therefore being different? We have no evidence to decide this question, or whether changes in isotopic discrimination account for any of the variations in our isotopic data.

There are also uncertainties in our inferred fluxes because of the coarse geographic division of the source components used in our inversion procedure. Our avoidance of longitudinal divisions is justified, we believe, not only because we lack stations to distinguish east-west variations, but also because the

variations in CO₂ that reflect significant interannual variations in sources and sinks east to west are too small to be established adequately at present precision of measurements and density of observing stations, even if data from all other measuring programs were used in the inversion. In the northern temperate zone, extracting east-west variability in terrestrial biospheric fluxes is made particularly difficult because large emissions of CO₂ from fossil fuel combustion strongly influence CO₂ gradients, in a manner that cannot be adequately predicted with existing transport models. Also isotopic data are of little value to separate these emissions from terrestrial biological fluxes.

In the north-south direction, more distinct CO₂ gradients are found for both concentration and ¹³C/¹²C ratio on large spatial scales, because north-south atmospheric mixing and transport are less vigorous than in the east-west direction. Nevertheless, the comparisons of results from different inversion studies, discussed in section 4, above, do not show close concordance in partitioning of the strength of zonally averaged sources and sinks of CO₂ between terrestrial biospheric and oceanic.

To challenge the findings of our inversion model we have employed sensitivity tests, discussed in Article III. We find that model results are insensitive to changes in many of its specifications, such as the exact position of boundaries between zones (tested by changing latitudinal boundaries by ±8°) and changes in long term average isotopic discrimination of plants. Using isotopic data in the fitting procedure for only the 5 stations that have records back to 1981, or omitting all data for Christmas Island, does not affect the simulation of fluxes significantly. Changing the wind fields from 1986 to 1987, or to a sequence of years, or altering the specified distribution of fossil fuel emission with latitude causes larger changes, but still does not change the general character of the results.

Most serious is the sensitivity of the results to the concentration and ¹³C/¹²C ratio given by data for La Jolla, California. Inferred fluxes for our standard case (Article II, Figure 4) and preferred case (Figure 5, above) differ substantially (Article III, Figure 15a) even though the only change in their calculation in the latter case is to remove the terrestrial source components from the grid box for La Jolla (see Article III, subsection 5.3).

5.4 Uncertainty in simulated regional fluxes

Given the uncertain magnitudes of our inferred regional fluxes, just discussed, how much information can we derive from our CO₂ data? The best known CO₂ exchange flux in our study is the sum of the global terrestrial and oceanic fluxes, evaluated directly from globally averaged atmospheric CO₂ measurements, as discussed in section 3, above. Beginning with this fact we have adopted a "top down" approach to appraise our findings (cf. Article I, subsection 7.3). We accept the estimates of errors reported in the Second Assessment Report of the IPCC for the 1980's [Houghton et al., 1996], expressed at the 90% confidence interval (see Article I, Table 3), and assumed to apply also to the 1990's.

The sum of the terrestrial and oceanic global fluxes is evidently established within 0.5 PgC yr⁻¹, as the difference

between industrial CO₂ emissions (mainly from fossil fuel combustion), known according to the IPCC assessment to within 0.5 PgC yr⁻¹, and the rate of increase in atmospheric CO₂ concentration, known to within 0.2 PgC yr⁻¹. Thus, since the global oceanic flux is known within 0.8 PgC yr⁻¹, the global net biospheric flux, in spite of the "missing CO₂ problem", is evidently known within about 0.9 PgC yr⁻¹, established by difference between the combined flux and the oceanic flux.

Averaging over our entire record period (1981-1999, see Table 2), we find a global terrestrial biospheric sink of -0.5 PgC yr⁻¹. The northern temperate zone is found to be a much stronger sink of -1.7 PgC yr⁻¹. The remaining three zones therefore are together a terrestrial source of 1.2 PgC yr⁻¹. However, the northern temperate sink is uncertain by as much as 2 PgC yr⁻¹, as discussed in subsection 5.3 above, and therefore the tendency for the other three regional terrestrial fluxes to be sources is equally uncertain.

TABLE 2
ESTIMATES OF SOURCES AND SINKS, IN PGC YR⁻¹, FOR 5 LATITUDINAL ZONES^a

1981-1989	bio	oce	bio+oce	foss	atm
47-90N	0.360	-0.738	-0.378	1.740	
23.5-47N	-1.348	-1.095	-2.443	3.049	
23.5S-23.5N	0.908	0.688	1.596	0.484	
23.5-47S	-0.137	-0.608	-0.745	0.188	
47-90S	-0.002	-0.247	-0.248	0.001	
Global	-0.218	-2.000	-2.218	5.462	3.243
1990-1996	bio	oce	bio+oce	foss	atm
47-90N	0.055	-0.690	-0.635	1.725	
23.5-47N	-2.105	-1.010	-3.115	3.636	
23.5S-23.5N	2.004	0.395	2.399	0.637	
23.5-47S	-1.095	-0.599	-1.693	0.229	
47-90S	-0.011	-0.239	-0.239	0.002	
Global	-1.152	-2.142	-3.294	6.228	2.934
1990-1999	bio	oce	bio+oce	foss	atm
47-90N	-0.106	-0.708	-0.814	1.723	
23.5-47N	-2.094	-1.041	-3.135	3.777	
23.5S-23.5N	2.598	0.304	2.902	0.674	
23.5-47S	-1.173	-0.642	-1.814	0.239	
47-90S	-0.012	-0.274	-0.274	0.002	
Global	-0.786	-2.361	-3.147	6.414	3.266
1981-1999	bio	oce	bio+oce	foss	atm
47-90N	0.115	-0.722	-0.608	1.731	
23.5-47N	-1.740	-1.067	-2.807	3.432	
23.5S-23.5N	1.798	0.486	2.283	0.584	
23.5-47S	-0.682	-0.626	-1.308	0.215	
47-90S	-0.007	-0.261	-0.261	0.002	
Global	-0.517	-2.190	-2.707	5.963	3.255

^a Fluxes to the atmosphere are positive numbers. bio = terrestrial biospheric reservoir, oce = ocean reservoir, foss = CO₂ from fossil fuel combustion and cement manufacture, atm = rate of increase of atmospheric CO₂.

Some findings of our simulations are more secure. Errors in simulating the northern temperate terrestrial flux, owing to bias in model prediction of atmospheric CO_2 , for example at La Jolla, is probably similar for each decade, so that our finding that both temperate sinks and the tropical source increased between the 1980's and 1990's is more likely to be correct than the long term average magnitudes of these regional fluxes.

If we ignore interannual variability in $^{13}\text{C}/^{12}\text{C}$ data in our simulation of CO_2 fluxes, the predicted variability of the terrestrial biospheric flux, though strongly reduced in the tropical zone, changes only slightly elsewhere, as shown above in Figure 6. As discussed above in subsection 3.2, either the tropical oceanic flux has actually varied significantly in opposite phase to the biospheric flux, as shown in Figure 5, or our neglect to consider interannual variability in isotopic discrimination of plants has led to our inferring an exaggerated biospheric signal. The latter possibility should not prevent our probing the cause of interannual variability of inferred fluxes in the tropical zone, however, because the close association of our data for both atmospheric CO_2 concentration and $^{13}\text{C}/^{12}\text{C}$ ratio is strong evidence that both fluxes have been closely phased with El Niño events and other episodes of strong warming.

In Figure 13, the tropical terrestrial biospheric flux that we calculate is compared with tropical land surface air temperature anomalies and with tropical precipitation near the times of El Niño events in 1982-3, 1987-8, and 1997-8, which were the strongest events over the past two decades [Slingo and Annamalai, 2000]. But establishing causal relationships for these three events is not straight forward because tropical temperature anomalies and precipitation are anticorrelated. Both high temperatures and low precipitation associated with each event, are likely to cause a reduction in net terrestrial uptake of CO_2 : high temperatures increasing autotrophic and heterotrophic respiration of plants and soils, low precipitation suppressing net primary production. Associated with climatic stress, isotopic discrimination may diminish as well. If so, our assumption of invariant discrimination has caused an exaggerated signal in the inferred fluxes shown in Figure 13. Nevertheless, the qualitative relationship of terrestrial flux to these climatic factors, over El Niño cycles, should not be distorted by uncertainty in modeling this discrimination.

If the climatic correlations just discussed hold generally they should be seen in the predictions of process-based terrestrial biosphere models, but analysis of cause and effect is handicapped by the close anticorrelation of temperature and precipitation. However, from 1990 through 1993 this relationship broke down. First, in 1990-1991, the tropics experienced an El Niño-like warming with only a minor tendency for drought. Then ensued a sharp cooling, associated with the eruption of the volcano, Pinatubo, with low precipitation, especially in 1992. Instead of cool, wet conditions replacing hot, dry conditions, typical of El Niño cycles, it was cool and dry. As shown in Figure 9, the process-based model, HRBM (purple curve), shows a pattern similar to that for strong El Niño events, a high flux predicted near the beginning of 1990. The other three models, IBIS, LPJ, and TEM, show high fluxes later, near the beginning of 1992 when precipitation

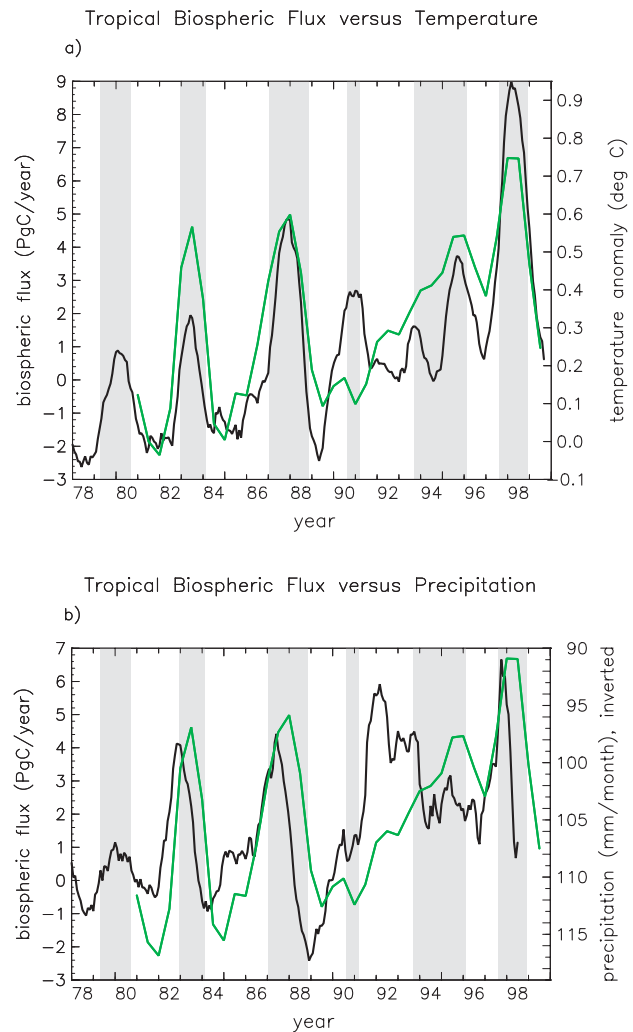


Fig. 13. Net annual CO_2 exchange flux, in PgC yr^{-1} , positive to the atmosphere, for the tropical terrestrial biosphere, as shown in Figure 5 (green curves), compared with annual average temperature and precipitation for the same zone (black curves). **Panel a:** Surface air temperature anomaly, in $^{\circ}\text{C}$, derived from gridded data of Jones et al. [1994, and website communication]. **Panel b:** precipitation in mm per month, from Hulme [1992, and website communication]. Gray bars as in Figure 5.

was lowest. The predictions of models, IBIS and TEM, are closely phased with precipitation, peak fluxes near the time of least precipitation. By inversion we calculate a weak flux signal similar to IBIS and TEM near 1992. Thus the models do not all agree on which climate variable is more important to forcing the tropical biosphere. However, three of them favor precipitation, consistent with the correlation that we find by inversion for this period of cool, dry conditions.

For the other zones, comparisons are more difficult because there are no striking patterns similar to those in the tropics and little agreement among the process-based model predictions. In the north temperate zone, 30° to 45°N , the patterns of the IBIS and LPJ models (see Figure 10) show some agreement with our results, but with lesser variability, as also seen in our comparison with Schimel et al. [2000] (see Figure 11).

In summary, except that all terrestrial biospheric models show similar tropical patterns associated with strong El Niño events, there is little concordance in the variability of predicted

fluxes. Decadal average fluxes hover about zero, whereas our inversion model, and to a considerable degree other inversion models cited in section 4, infer persistent zonal sources and sinks. If the fluxes from inversion models are more correct than from process-models, the latter, as presently formulated, must be insensitive to the full range of variability in external factors such as temperature and precipitation.

5.5 Significance of findings

Our simulations of carbon cycle fluxes, inferred from atmospheric CO₂ data by inversion, indicate that the terrestrial biosphere has been a sink for atmospheric CO₂ in temperate regions, and most of the time a source elsewhere. These findings imply imbalances in the terrestrial carbon cycle which are too far from steady state conditions to be permanent features. Indeed, the temperate sinks appear to be increasing.

Sustained increases in net uptake of atmospheric CO₂ suggest that plant growth has been stimulated ("fertilized") by rising atmospheric CO₂ concentrations, a possibility of special interest because it may counteract this rise. Attempts to explain the budget of atmospheric CO₂ from the beginning of the industrial era, indeed, suggest that the rise would have been greater in the absence of a fertilization effect, and we have therefore allowed for it in our deconvolution calculations of the global carbon cycle in Article I.

Fertilized growth of land vegetation should not be restricted to the temperate zones, however, and our finding sources elsewhere much of the time suggests the influence of additional factors. Indeed, on the short term, we discern an overriding climatic effect in the northern polar zone with respect to net biospheric CO₂ flux. Here, over the 1980's, increases in the seasonal amplitudes of observed atmospheric CO₂ [Keeling et al., 1996] and of remotely-sensed vegetative index (NDVI) data, indicate increasing plant growth [Myneni et al., 1997]. Nevertheless, we find an increasing net source of atmospheric CO₂ (see Figure 5), evidence that the sink from greater growth was less than CO₂ released to the air by respiration. Probably increasing net primary production and heterotrophic respiration both contributed to an increase in amplitude of the seasonal cycle. Indeed, there is evidence from field studies that boreal forests and tundra may grow more rapidly above ground and still be a source of CO₂ in warmer years, owing to enhanced soil respiration [Goulden et al., 1998]. Adding still more complexity to analysis of net exchange fluxes, increasing terrestrial biospheric uptake of atmospheric CO₂ may result from increased length of growing season [Keeling et al., 1996] or by fertilization with nitrogen [Holland et al., 1997], as well as by fertilization caused by higher ambient CO₂.

Increasing temperature, with which the increasing seasonal cycle, just described, was found to correlate [Keeling et al. 1996], is a factor which may explain longer term variability in terrestrial CO₂ fluxes. In the tropics, the increase in source that we find from the 1980's to the 1990's, from 0.9 PgC yr⁻¹ to 2.3 PgC yr⁻¹ (see Table 2) could well be related to a remarkable increase in temperature recently (Figure 13a), reinforced by a strong concurrent drought condition (Figure 13b). Whether the El Niño of 1998 was extraordinarily warm

owing to some natural factor related to the internal dynamics of the coupled atmospheric-ocean circulation system, or owing to an enhanced greenhouse effect, it was the warmest El Niño event globally since instrumental records began, as is evident in the plot of Article I, Figure E1. For the time of this event, we find the largest simulated regional terrestrial biospheric net flux over the past two decades for any region. As discussed in section 4, the relationship of flux strength with the El Niño cycle is likely to hold even if our simulations have exaggerated tropical fluctuations by assuming constant isotopic discrimination of plants, because, as we argue in subsection 5.3, above, discrimination, if it varies, probably does so in phase with this cycle. Our inferred patterns in tropical biospheric flux should therefore not depend on whether discrimination is constant or variable.

Thus our calculated terrestrial fluxes imply a strong sensitivity of the polar and tropical terrestrial biosphere to climatic factors. In the temperate zones they also suggest sequestration of atmospheric CO₂ by plant growth fertilized by atmospheric CO₂. Both these natural and anthropogenic processes probably occur in all zones, but climatic processes appear to have overridden sequestration in the polar zone, owing to a reduction in extreme cold, and in the tropical zone, owing to an approach to intolerably warm temperatures.

6. CONCLUSIONS

We have analyzed atmospheric CO₂ data by an inverse procedure with the objective to improve and extend estimates of atmospheric CO₂ exchange fluxes with the land and oceans. A nearly 20-year record of paired measurements of the concentration and ¹³C/¹²C ratio allows terrestrial biospheric and oceanic fluxes to be distinguished over an extended period. Ability to distinguish is limited, however, by uncertainty in prescribing isotopic fractionation, and on long term average, to establish oceanic uptake of CO₂ attending rising concentrations in the atmosphere.

We are not hindered, however, from investigating short-term interannual variability in CO₂ exchange, and the only problematic uncertainty in prescribing isotopic fractionation is possible temporal variability in the preference of plants to take up the light isotope, ¹²C, during photosynthesis. By carrying out an alternate inversion calculation in which isotopic data are not used to determine variability in fluxes, we find that these data strongly influence variability only in the tropics, and probably only to reduce it, not to alter its timing.

We have sought to establish how much short-term interannual variability in exchange fluxes is inferred solely from observed interannual variability in atmospheric CO₂ concentration and ¹³C/¹²C ratio. This focus is partially motivated by expediency. Because adequate data are not yet available, we have been obliged to leave out of consideration interannual variability in wind fields that determine atmospheric transport of CO₂, and interannual variability in net primary production of land plants, that can be estimated from remotely sensed vegetative index data (NDVI). Nevertheless our limited approach provides a ground base for future judging of more complicated simulations, to be carried out when supporting data become

available. Also, sensitivity tests, described in Article III, indicate that neglected causes of variation, except interannually variable atmospheric transport and isotopic discrimination by plants, can explain only a small part of the variability that we find.

In summary, variability in exchange fluxes of atmospheric CO₂ appears to be more substantial than predicted by process-based models or reported in other inversion studies, and shows substantial evidence of climate forcing. We have found substantial and increasing sinks of atmospheric CO₂ in the temperate zones of both hemispheres. These sinks, arguably, could reflect sequestration of CO₂ under climatic conditions favorable to stimulation of plant growth by rising atmospheric CO₂ in spite of temperatures that were warmer than in any previous decade of the 20th century. For polar and tropical zones, we find sources of atmospheric CO₂, suggesting that warmer temperatures, and in some regions drought conditions as well, have overridden any tendency for such sequestration.

ACKNOWLEDGMENT

Funding for this research was provided by the U.S. National Aeronautics and Space Administration, U.S. National Science Foundation, and U.S. Department of Energy by grants NASA NAG5-3469, NSF ATM 97-11882, NSF OCE 97-25995, and DOE DE-FG03-95ER62075, and by the Office of the Director of the Scripps Institution of Oceanography.

REFERENCES

- [1] Battle, M. M. L. Bender, P. P. Tans, J. W. C. White, J. T. Ellis, T. Conway, and R. J. Francey, Global carbon sinks and their variability inferred from atmospheric O₂ and $\delta^{13}C$. *Science*, 287, 2467-2470, 2000.
- [2] Conway, T. J., P. P. Tans, L. S. Waterman, and K. W. Thoning, Evidence for interannual variability of the carbon cycle from the National Oceanic and Atmospheric Administration Climate Monitoring and Diagnostics Laboratory Global Air Sampling Network, *J. Geophys. Res.-Atmos.*, 99, 22831-22855, 1994.
- [3] Framework Convention on Climate Change. <http://www.unfccc.de/resource/cop3.html>. FCCC/CP/1997/7/Add. 1, Decision 1/CP.3, Annex, 7-30, 1997.
- [4] Francey, R. J., P. P. Tans, C. E. Allison, I. G. Enting, J. W. C. White, and M. Trolier, Changes in oceanic and terrestrial carbon uptake since 1982, *Nature*, 373, 326-330, 1995.
- [5] Goulden, M. L., S. C. Wofsy, J. W. Harden, S. E. Trumbore, P. M. Crill, S. T. Gower, T. Fries, B. C. Daube, S. M. Fan, D. J. Sutton, A. Bazzaz, and J. W. Munger, Sensitivity of boreal forest carbon balance to soil thaw, *Science*, 279, 214-217, 1998.
- [6] Heimann, M. Atmospheric Inversion Calculations Performed for IPCC TAR, Chapter 3 (Carbon Cycle), in preparation, 2000.
- [7] Holland et al., [1997] (see Article II!)
- [8] Houghton, J. T., L. G. Meira Filho, B. A. Callander, N. Harris, A. Kattenberg, and K. Maskell, eds., *Climate Change 1995, The Science of Climate Change, Contribution of Working Group I to the Second Assessment Report of the Intergovernmental Panel on Climate Change*, 572 pages, Cambridge University Press, Cambridge, 1996.
- [9] Hulme, M., A 1951-80 global land precipitation climatology for the evaluation of general circulation models, *Climate Dynamics*, 7, 57-72, 1992.
- [10] Jones, P. D., Hemispheric surface air temperature variations: a reanalysis and an update to 1993, *J. Climate*, 7, 1794-1802, 1994.
- [11] Keeling, C. D., R. B. Bacastow, A. F. Carter, S. C. Piper, T. P. Whorf, M. Heimann, W. G. Mook, and H. Roeloffzen, A three-dimensional model of atmospheric CO₂ transport based on observed winds: 1. Analysis of observational data, in *Aspects of Climate Variability in the Pacific and the Western Americas, Geophysical Monograph, vol. 55*, edited by D. H. Peterson, pp. 165-236, AGU, Washington, D. C., 1989a.
- [12] Keeling, C. D., S. C. Piper, and M. Heimann, A three-dimensional model of atmospheric CO₂ transport based on observed winds: 4. Mean annual gradients and interannual variations, in *Aspects of Climate Variability in the Pacific and the Western Americas, Geophysical Monograph, vol. 55*, edited by D. H. Peterson, pp. 305-363, AGU, Washington, D. C., 1989b.
- [13] Keeling, C. D., J. F. S. Chin, and T. P. Whorf, Increased activity of northern vegetation inferred from atmospheric CO₂ measurements, *Nature*, 382, 146-149, 1996.
- [14] Keeling, C. D., S. C. Piper, R. B. Bacastow, M. Wahlen, T. P. Whorf, M. Heimann, and H. A. Meijer, Exchanges of atmospheric CO₂ and ¹³CO₂ with the terrestrial biosphere and oceans from 1978 to 2000. I. Global aspects, SIO Reference Series, No. 01-06 (Revised from SIO Reference Series, No. 00-21), Scripps Institution of Oceanography, San Diego, 2001.
- [15] Keeling, C. D., and S. C. Piper, Exchanges of atmospheric CO₂ and ¹³CO₂ with the terrestrial biosphere and oceans from 1978 to 2000. IV. Critical overview, SIO Reference Series, No. 01-09 (Revised from SIO Reference Series, No. 00-24), Scripps Institution of Oceanography, San Diego, 2001.
- [16] McGuire, A. D., S. Sitch, J. S. Clein, R. Dargaville, G. Esser, J. Foley, M. Heimann, F. Joos, J. Kaplan, D. W. Kicklighter, R. A. Meier, J. M. Melillo, B. Moore, I. C. Prentice, N. Ramankutty, T. Reichenau, A. Schloss, H. Tian, L. J. Williams, and U. Wittenberg, Carbon balance of the terrestrial biosphere in the twentieth century: Analyses of CO₂, climate and land use effects with four process-based ecosystem models, *Global Biogeochemical Cycles*, 15, 183-206, 2001.
- [17] Masarie, K. A. and P. P. Tans, Extension and integration of atmospheric carbon dioxide data into a globally consistent measurement record, *J. Geophys. Res.-Atmos.*, 100, 11593-11610, 1995.
- [18] Myneni, R. B., C. D. Keeling, C. J. Tucker, G. Asrar, and R. R. Nemani, Increased plant growth in the northern high latitudes from 1981 to 1991, *Nature* 386, 698-702, 1997.
- [19] Piper, S. C., C. D. Keeling, M. Heimann, and E. F. Stewart, Exchanges of atmospheric CO₂ and ¹³CO₂ with the terrestrial biosphere and oceans from 1978 to 2000. II. A three-dimensional tracer inversion model to deduce regional fluxes, SIO Reference Series, No. 01-07 (Revised from SIO Reference Series, No. 00-22), Scripps Institution of Oceanography, San Diego, 2001a.
- [20] Piper, S. C., C. D. Keeling, and E. F. Stewart, Exchanges of atmospheric CO₂ and ¹³CO₂ with the terrestrial biosphere and oceans from 1978 to 2000. III. Sensitivity tests, SIO Reference Series, No. 01-08 (Revised from SIO Reference Series, No. 00-23), Scripps Institution of Oceanography, San Diego, 2001b.
- [21] Rayner, P. J., I. G. Enting, R. J. Francey, and R. Langenfelds, Reconstructing the recent carbon cycle from atmospheric CO₂, $\delta^{13}C$ and O₂/N₂ observations, *Tellus 51B*, 213-232, 1999a.
- [22] Rayner, P. J., R. M. Law, and R. Dargaville, The relationship between tropical CO₂ fluxes and the El Niño-Southern Oscillation, *Geophys. Res. Lett.*, 26, 493-496, 1999b.
- [23] Schimel, D., J. Melillo, H. Q. Tian, A. D. McGuire, D. Kicklighter, T. Kittel, N. Rosenbloom, S. Running, P. Thornton, D. Ojima, W. Parton, R. Kelly, M. Sykes, R. Neilson, and B. Rizzo, Contribution of increasing CO₂ and climate to carbon storage by ecosystems in the United States, *Science*, 287, 2004-2006, 2000.
- [24] Slingo, J. M. and H. Annamalai, 1997: The El Niño of the century and the response of the Indian summer monsoon, *Monthly Weather Review*, 128, 1178-1197, 2000.
- [25] Trolier, M., J. W. C. White, P. P. Tans, K. A. Masarie, and P. A. Gemery, Monitoring the isotopic composition of atmospheric CO₂ - measurements from the NOAA Global Air Sampling Network. *J. Geophys. Res.-Atmos.*, 101, 25897-25916, 1996.